Self-Assembly and (Hydro)gelation Triggered by Cooperative π-π and Unconventional CH ···X Hydrogen Bonding Interactions

ARTICLE *in* ANGEWANDTE CHEMIE INTERNATIONAL EDITION · JANUARY 2014

Impact Factor: 11.26 · DOI: 10.1002/anie.201307806 · Source: PubMed

6 AUTHORS, INCLUDING:

Maria Jose Mayoral
Universidad Autónoma de Madrid
29 PUBLICATIONS **333** CITATIONS
SEE PROFILE

Katharina Edkins
Durham University
36 PUBLICATIONS **406** CITATIONS
SEE PROFILE

Vladimir Stepanenko
University of Wuerzburg
65 PUBLICATIONS **2,055** CITATIONS
SEE PROFILE

Gustavo Fernández
University of Wuerzburg
45 PUBLICATIONS **1,207** CITATIONS
SEE PROFILE

Weak Interactions

DOI: 10.1002/anie.201307806

Self-Assembly and (Hydro)gelation Triggered by Cooperative π–π and Unconventional C–H···X Hydrogen Bonding Interactions**

*Christina Rest, María José Mayoral, Katharina Fucke, Jennifer Schellheimer, Vladimir Stepanenko, and Gustavo Fernández**

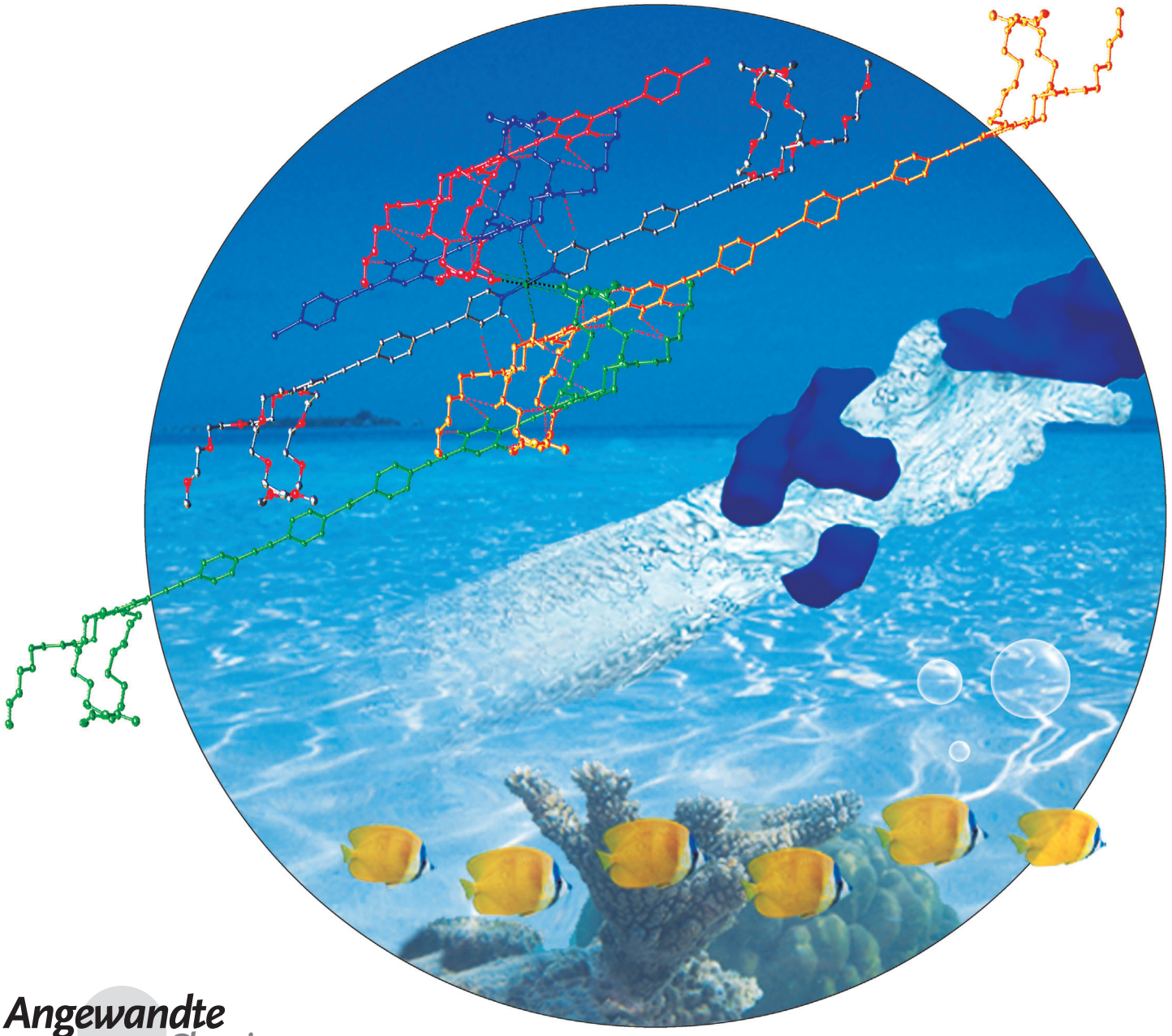

Abstract: *Weak C–H···X hydrogen bonds are important stabilizing forces in crystal engineering and anion recognition in solution. In contrast, their quantitative influence on the stabilization of supramolecular polymers or gels has thus far remained unexplored. Herein, we report an oligophenyleneethynylene (OPE)-based amphiphilic Pt^{II} complex that forms supramolecular polymeric structures in aqueous and polar media driven by π–π and different weak C-H···X (X = Cl, O) interactions involving chlorine atoms attached to the Pt^{II} centers as well as oxygen atoms and polarized methylene groups belonging to the peripheral glycol chains. A collection of experimental techniques (UV/Vis, 1D and 2D NMR, DLS, AFM, SEM, and X-Ray diffraction) demonstrate that the interplay between different weak noncovalent interactions leads to the cooperative formation of self-assembled structures of high aspect ratio and gels in which the molecular arrangement is maintained in the crystalline state.*

The occurrence of multiple weak C–H···X interactions involving electronegative atoms, anions, or π-systems is a phenomenon of high relevance in numerous natural processes, such as membrane transport, protein–ligand interactions, and drug–receptor recognition.[1] These weak hydrogen-bonding interactions[2] are largely recognized as important forces in the area of crystal engineering.[3] In recent years, C–H···X bonds have also been exploited as additional binding sites[4] or as relevant weak noncovalent interactions[5] in anion recognition by discrete preorganized receptors. In contrast, the use of these forces to stabilize self-assembled structures in solution or gel-phase materials has remained unexplored to date.

Herein, we show for the first time that cooperative π–π and multiple unconventional C–H···X hydrogen-bonding interactions are strong enough to induce the supramolecular polymerization and (hydro)gelation of an amphiphilic Pt^{II} system.

The design of this complex was originally motivated by the fact that halogens, when bound to metal ions, turn into sufficiently strong hydrogen-bond acceptors[6] that their interaction with polarized C–H hydrogen-bonding donors becomes favorable.[7] Recent studies from our group highlight that chlorine atoms coordinated to Pd^{II} ions can also play a significant role in the stabilization of self-assembled structures.[8] With these precedents in mind, we conceived an amphiphilic Pt^{II} complex **2** in which two hydrophobic oligophenyleneethynylene (OPE)[9] scaffolds featuring three hydrophilic triethylene glycol (TEG) chains each are coordinated to a central Pt^{II} ion through pyridine rings (Scheme 1).[10] Our system satisfies the above prerequisites,

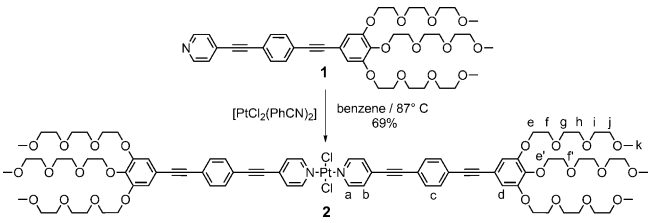

Scheme 1. Structural formula of the OPE-based ligand (**1**) and Pt^{II} complex (**2**).

as it features, besides a relatively large aromatic surface, a Cl-Pt^{II}-Cl fragment and a large number of methylene groups polarized by electronegative oxygen heteroatoms that can potentially participate in weak hydrogen bonding. We thus expected **2** to self-assemble by a combination of cooperative C–H···X and π–π interactions, given that the presence of sterically demanding Cl atoms and up to six bulky TEG chains would hinder the stacking of the monomeric units in a parallel fashion,[11] and consequently, the occurrence of metallophilic Pt···Pt interactions.[12]

The amphiphilic Pt^{II} complex **2** can be readily obtained in 69% yield by a complexation reaction between pyridine-based ligand **1** and $[PtCl_2(PhCN)_2]$ in benzene at 87 °C (Scheme 1, for characterization details see the Supporting Information).[13]

The absorption spectrum of **1** exhibits a maximum at approximately 332 nm in a wide range of solvents of different polarity (Figure S1 in the Supporting Information). In water, however, a small red-shifted shoulder at approximately 380 nm becomes visible (Figure 1a and Figure S1). This observation, along with the appearance of a low-intensity red-shifted maximum in emission studies (Figure S2), suggest stacking of the aromatic OPE units.[14] Temperature-dependent UV/Vis studies (3.5×10^{-5} M, 279–327 K, water) show a simultaneous bathochromic shift of the absorption maximum from 326 to 335 nm and appearance of a shoulder at 380 nm upon decreasing temperature (Figure 1a). The cooling curve obtained by monitoring the spectral changes extracted from temperature-dependent experiments at 300 nm is sigmoidal and indicates that **1** self-assembles in a non-cooperative fashion in water (Figure 1a, inset), affording an association constant of $4.8 \times 10^4\,M^{-1}$ (Figure S3 and Table S1).[15] The absence of additional intermolecular interactions other than π-stacking appears to be responsible for this non-cooperative behavior that ultimately results in the formation of aggregates of relatively low size (ca. 140 nm), as extracted from dynamic light scattering (DLS) experiments (Figure S4). Transmission electron microscopy (TEM) studies reveal the formation of worm-like aggregates with a regular width (1.8 ± 0.2 nm) and lengths of several tens of nanometers

[*] C. Rest, Dr. M. J. Mayoral, J. Schellheimer, Dr. V. Stepanenko, Dr. G. Fernández
Institut für Organische Chemie and Center for Nanosystems Chemistry, Universität Würzburg
Am Hubland, 97074 Würzburg (Germany)
E-mail: gustavo.fernandez@uni-wuerzburg.de
Homepage: http://www-organik.chemie.uni-wuerzburg.de/lehr-stuehlearbeitskreise/fernandez
Dr. K. Fucke
Institut für Anorganische Chemie, Universität Würzburg
Am Hubland, 97074 Würzburg (Germany)

[**] We thank Prof. Frank Würthner for many helpful discussions and his support, Ana Reviejo for graphic design, and the Alexander von Humboldt Foundation for financial support (Sofja Kovalevskaja Program).

Supporting information for this article is available on the WWW under http://dx.doi.org/10.1002/anie.201307806.

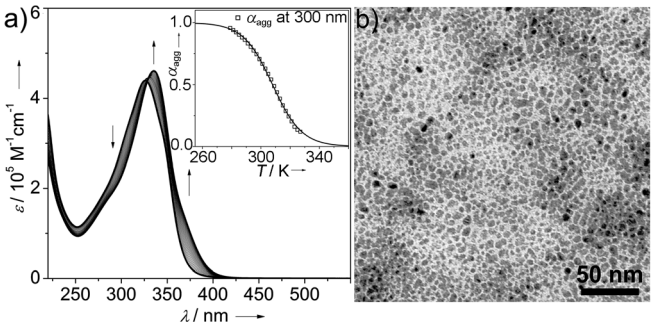

Figure 1. a) Temperature-dependent UV/Vis experiments of **1** (3.5×10^{-5} M, 279–327 K) in water. Arrows indicate the spectral changes upon decreasing temperature. Inset: Fraction of aggregated species (α_{agg}) against *T* and fit of the spectral changes at 300 nm to the isodesmic model. b) TEM micrograph of **1** onto a carbon-coated copper grid.

that subsequently entangle into a porous network (Figure 1b and Figure S5). These are most likely formed by the π-stacking of the OPE units with a small rotation angle to avoid steric repulsions between the bulky TEG chains.

Coordination of the pyridine-based ligand **1** to a Cl-Pt^{II}-Cl fragment leads to notable changes in the optical and supramolecular properties. The self-assembly of amphiphilic Pt^{II} complex **2** can be readily monitored by the naked eye, as the transition from monomeric to aggregated species is accompanied by a color change from pale to deep yellow (Figure 2a). UV/Vis studies show the presence of a transition centered at approximately 350–354 nm in most organic solvents even at millimolar concentration, characteristic of molecularly dissolved species (Figure S6). However, the color of the solutions of **2** in alcohols and water turn deep yellow and a red-shift of the absorption maximum to approximately 370 nm takes place, which can be attributed to the formation of self-assembled species (Figure 2a and Figure S6). Above a certain concentration, stable yellow gels are formed in various alcohols and water (see Supporting Information), most likely driven by strong solvophobic interactions and an efficient solvation of the polar TEG chains of **2** in these media.

Figure 2b,c show the atomic force microscopy (AFM) images of diluted gel solutions of **2** in ethanol (4.9×10^{-3} M) and water (2.2×10^{-3} M) onto mica. For both gels, the images reveal a network consisting of long flexible nanofibers with a consistent diameter of 5.8 ± 0.4 nm and lengths of up to 500 nm (Figure 2b,c, Figures S7 and S8). Comparable networks of aggregates are also visualized by SEM studies (Figures S9 and S10). The fact that in alcohols and water both the morphology of the gel nanofibers and UV/Vis spectra of the gel materials are very similar suggests an analogous arrangement of the monomeric units of **2** in both media.

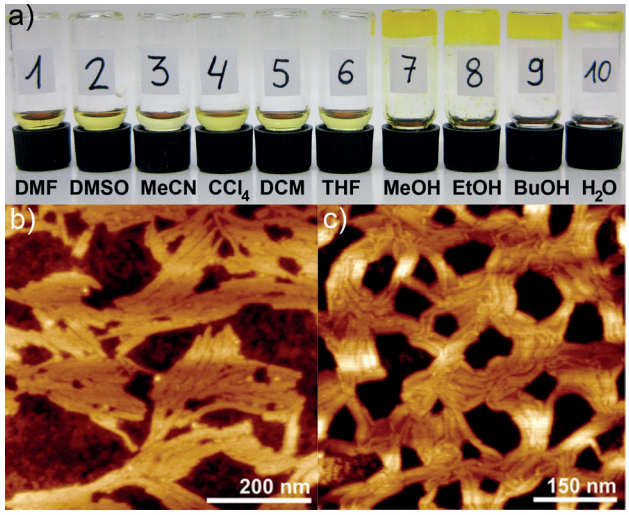

Figure 2. a) Photograph illustrating the color change associated to the monomer-aggregate/gel transition of **2** in different solvents at 9 mM. AFM images obtained by drop-casting diluted gel solutions of **2** in water (b) and ethanol (c) onto mica.

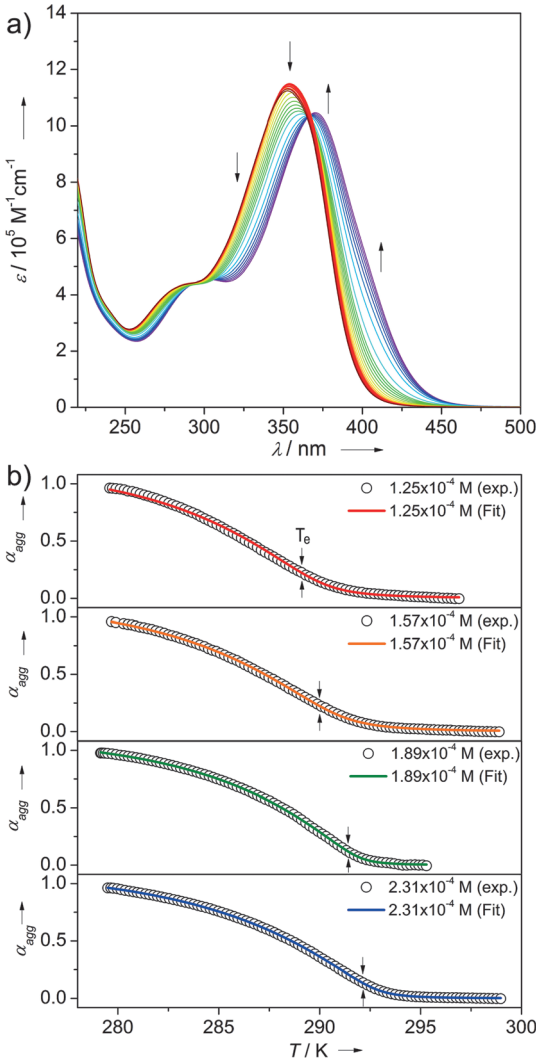

Figure 3. a) Temperature-dependent UV/Vis experiments of **2** (MeOH/H_2O (70:30), 1.28×10^{-4} M). Arrows indicate the spectral changes upon decreasing temperature. b) Cooling curves obtained by monitoring the absorption of **2** in MeOH/H_2O (70:30) at 420 nm at four different concentrations. Colored lines represent the fits to the ten Eikelder-Markvoort-Meijer cooperative model.

Temperature-dependent UV/Vis experiments in water at 1.02×10^{-5} M show that the transition at 370 nm undergoes negligible changes upon increasing temperature, indicating that the molecules of **2** are strongly bound in this medium (Figure S11a). The extension of the aromatic surface upon metal coordination as well as the involvement of the Cl-Pt^{II}-Cl fragment in intermolecular interactions are most likely responsible for the enhanced degree of aggregation of **2** in water compared to that of ligand **1**. However, the monomer–aggregate equilibrium can be fully tracked by addition of a suitable amount of methanol to an aqueous solution of **2** (see Figure S11).[16] Figure 3a shows the temperature-dependent UV/Vis experiments of **2** in methanol/water (70:30) at 1.28×10^{-4} M. Above 313 K, an absorption at 353 nm corresponding to molecularly dissolved species can be observed. Upon decreasing temperature, depletion of this transition is accompanied by the emergence of a red-shifted band at 370 nm that is assigned to self-assembled species (Figure 3a). The cooling curves ($\lambda = 420$ nm; cooling rate $= 0.2$ K min^{-1}) extracted from these experiments at four different concentrations are clearly non-sigmoidal and reminiscent of a phase transition (Figure 3b), which is a distinctive feature of cooperative supramolecular polymerization processes.[17] Analysis of the curves through a recently developed nucleation–elongation model[18] afforded excellent fits (Figure 3b and Figure S12). The self-assembly of **2** can be thus divided into a thermodynamically unfavorable dimerization process and a subsequent highly favorable elongation step. The enthalpy of elongation (ΔH_e) was calculated to be approximately -120 kJ mol^{-1}, the dimerization (K_2) and elongation (K) constants are 63.8 and approximately 8×10^{3} M^{-1} respectively, and the cooperativity factor (σ), described as $\sigma = K_2/K$, is 7.9×10^{-3} (Table S3).

To shed some light on the driving force of this cooperative self-assembly process we have performed 1D and 2D NMR spectroscopic studies. As the ^{1}H NMR spectra of **2** in D_2O is severely broadened as a result of a strong aggregation (Figure S14), we have chosen as a solvent CD_3OD. In this medium, an aggregation process similar to that in water takes place (see Figure S6c) however, the NMR signals are now sufficiently sharp. Concentration-dependent ^{1}H NMR spectroscopy experiments (CD_3OD, 400 MHz, 0.4–13 mM, 298 K) show a simultaneous shielding and broadening of all resonance signals upon increasing concentration (Figure S15), indicating that both aromatic and TEG units are strongly involved in the formation of self-assembled structures. Rotating-frame Overhauser Effect Spectroscopy (ROESY) NMR experiments show the absence of cross-peaks in CD_2Cl_2, a solvent in which **2** exists in a monomeric form (Figure S16). In contrast, multiple through-space coupling signals between protons which are in spatial proximity are in fact observed in CD_3OD (Figure S17).[19] Upon closer inspection, we noticed clear cross-peaks between protons (H_d) belonging to the outer phenylene rings and protons H_a and H_b of the pyridine units (Figure 4a). According to this coupling pattern, the only possible molecular arrangement is that in which one Cl-Pt^{II}-Cl fragment lies on top of the outer phenylene ring of the molecule immediately below in the stack, most likely stabilized by π–π and Cl···π interactions, as illustrated in Figure 4c. This structural proposition is clearly supported by all intramolecular (H_c···H_d and H_b···H_c) and intermolecular (H_a···H_c and H_b···H_c) cross-peaks observed in the ROESY spectrum (highlighted in red and green, respectively, in Figure 4a). Additionally, the appearance of coupling signals between most of the protons of the TEG chains (H_{e-k}) and protons H_{a-d} (Figure 4b) suggests that the TEG chains of one monomer should be wrapped around the aromatic core of a neighboring unit of **2**.

By slow evaporation of an aggregate solution of **2** in methanol, yellow single crystals suitable for X-ray diffraction could be obtained. The resulting crystal structure could be solved and refined in the triclinic space group $P\bar{1}$ with half a molecule in the asymmetric unit (Table S5 and Fig-

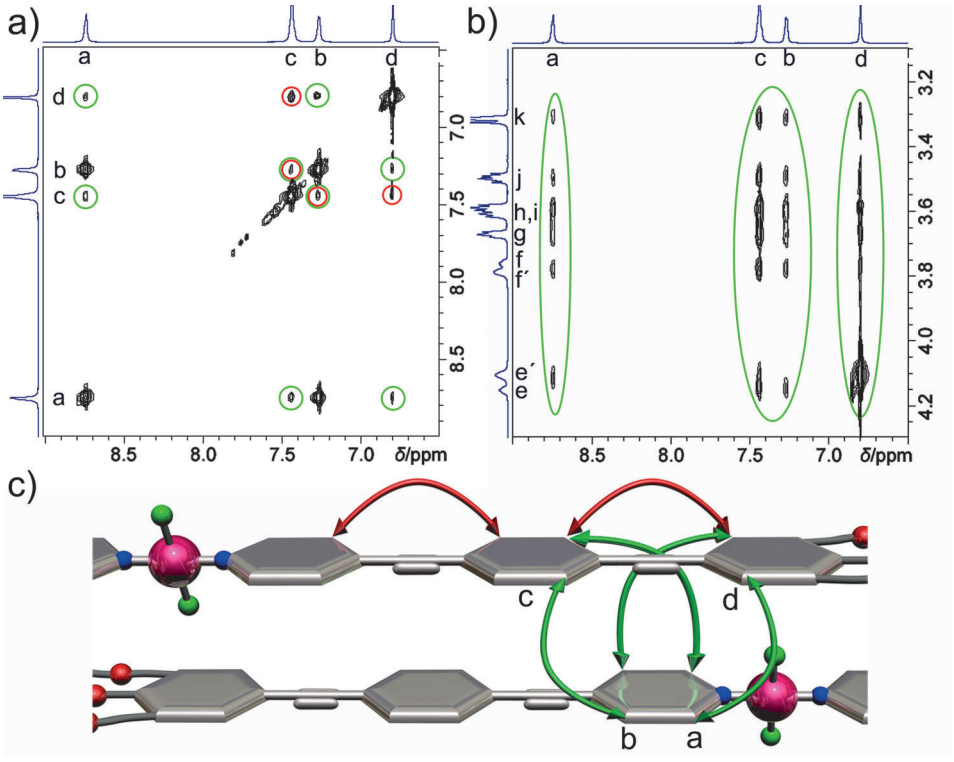

Figure 4. a,b) Selected areas of the ROESY NMR spectrum (CD_3OD, 600 MHz, 14.1 mM, 293 K) of **2**. The red and green circles highlight intra- and intermolecular through-space coupling signals, respectively. c) Representation of the molecular organization of **2** to form self-assembled structures on the basis of ROESY studies.

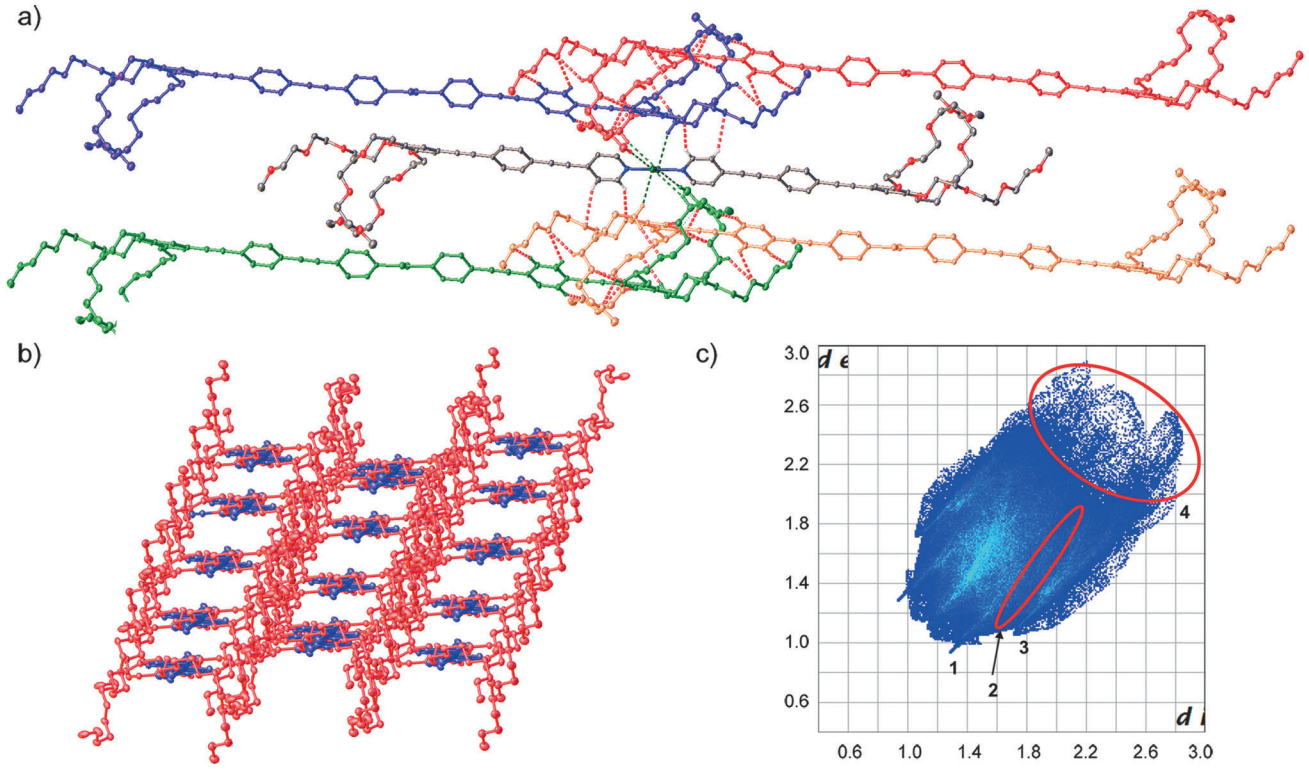

Figure 5. a) Packing of **2** driven by C–H···Cl (green) and C–H···O (red) hydrogen-bonding interactions. b) Overall packing of the crystal structure seen along the OPE units. OPEs (blue) and TEG chains (red). C gray, O red, N blue, Pt dark blue, Cl green, H white. Displacement ellipsoids are set at 50% probability, non-hydrogen-bonding hydrogen atoms in (a) and all hydrogen atoms in (b) are omitted for clarity. c) Hirshfeld surface fingerprint plot of **2**. Colors describe the frequency of a specific distance with blue being less frequent and light green being most common.

ure S20).[20] The presence of bulky Cl-Pt^{II}-Cl and TEG fragments forces the OPE units to pack in a slipped fashion through translationally stacked CH···π interactions (Figure 5a,b). This arrangement is supported by C–H···Cl and C–H···O hydrogen bonding interactions (Table S6). Each chlorine atom is involved in up to four C–H···Cl interactions with O-CH_2 groups belonging to the TEG chains of four different molecules, facilitating the growth of the structure in one dimension (see Figure 5a, green dotted lines).

A further growth is driven by multiple C–H···O interactions between three of the TEG chains of one molecule and another three TEG chains of a neighboring unit in an exotic "handshake-like" fashion, in part involving aromatic C–H groups (Figure 5a, red dotted lines). This crystalline packing perfectly matches the slipped molecular arrangement of **2** in solution and also explains all cross-peaks between most of the protons of the TEG chains (H_{e-k}) and protons H_{a-d} (see Tables S7–10) observed in ROESY studies. To visualize the interactions of this molecule, the Hirshfeld surface (Figure S21)[21] has been calculated and the corresponding fingerprint plot is shown in Figure 5c (see also Figure S22). Four regions show interesting features: Region 1 corresponds to C–H···O hydrogen bonds, which make a total of 16.6% of the surface. This percentage is relatively high for a single type of interaction and clarifies its importance in the self-assembly of **2**. These interactions are also the shortest contacts and can be assumed as the strongest interactions (see Table S6).[22] Slightly hidden is Region 2, which represents C–H···C and C–H···π short contacts. These interactions are considerably longer than the C–H···O hydrogen bonds and will thus not be as strong, but with 22.3% they present a large portion of the surface as well. With only 4.5% of the surface, C–H···Cl interactions (Region 3) are slightly less important for the overall stability of the crystal packing, even though they are of comparable length than the C–H···C interactions. However, these forces appear to be more relevant in solution and the gel state, as Pt^{II} complex **2** forms gels cooperatively whereas pyridine-based OPE precursor **1**, which lacks the Cl-Pt^{II}-Cl fragment, only forms small aggregates in a non-cooperative fashion. Finally, Region 4 shows that the crystal packing has relatively large voids that can be attributed to the dimensions and high degree of flexibility of the monomeric units.

To summarize, we have shown for the first time that cooperative π–π and multiple unconventional CH···X (X = O, Cl) hydrogen-bonding interactions are the driving force for supramolecular polymerization and (hydro)gelation processes.[23] Complementary UV/Vis, NMR spectroscopy, and X-ray studies demonstrate that the molecular arrangement of amphiphilic Pt^{II} complex **2** in solution bears close resemblance to that in the crystalline state. Understanding the relationship between molecular packing in crystals and aggregates is one of the biggest challenges that chemistry faces today.[24] Our results make clear that CH···X hydrogen bonding can also play an important role, not only in crystal

engineering and anion binding, but in the formation of supramolecular polymers and gels.

Received: September 5, 2013
Revised: October 14, 2013
Published online: December 18, 2013

Keywords: amphiphiles · cooperativity · supramolecular polymerization · X–H hydrogen bonds · π-conjugated systems

[1] a) H. T. Chifotides, K. R. Dunbar, *Acc. Chem. Res.* **2013**, *46*, 894 – 906; b) A. V. Jentzsch, A. Hennig, J. Mareda, S. Matile, *Acc. Chem. Res.* **2013**, DOI: 10.1021/ar400014r.

[2] a) G. R. Desiraju, *Angew. Chem.* **2011**, *123*, 52 – 60; *Angew. Chem. Int. Ed.* **2011**, *50*, 52 – 59; b) E. Arunan, G. R. Desiraju, R. A. Klein, J. Sadlej, S. Scheiner, I. Alkorta, D. C. Clary, R. H. Crabtree, J. J. Dannenberg, P. Hobza, H. G. Kjaergaard, A. C. Legon, B. Mennucci, D. J. Nesbitt, *Pure Appl. Chem.* **2011**, *83*, 1619 – 1636; c) B. P. Hay, V. S. Bryansev, *Chem. Commun.* **2008**, 2417 – 2428.

[3] a) R. Custelcean, *Chem. Soc. Rev.* **2010**, *39*, 3675 – 3685; b) T. Steiner, *Angew. Chem.* **2002**, *114*, 50 – 80; *Angew. Chem. Int. Ed.* **2002**, *41*, 48 – 76; c) G. R. Desiraju, T. Steiner, *The Weak Hydrogen Bond*, Oxford University Press, New York, **1999**.

[4] a) H. Maeda, Y. Bando, *Chem. Commun.* **2013**, *49*, 4100 – 4113; b) P. A. Gale, *Acc. Chem. Res.* **2011**, *44*, 216 – 226; c) P. Ballester, *Chem. Soc. Rev.* **2010**, *39*, 3810 – 3830; d) D. J. Mercer, S. J. Loeb, *Chem. Soc. Rev.* **2010**, *39*, 3612 – 3620; e) Y. Hua, A. H. Flood, *Chem. Soc. Rev.* **2010**, *39*, 1262 – 1271; f) J. W. Steed, *Chem. Soc. Rev.* **2009**, *38*, 506 – 519; g) C.-H. Lee, H. Miyaji, D.-W. Yoon, J. L. Sessler, *Chem. Commun.* **2008**, 24 – 34; h) D.-W. Yoon, D. E. Gross, V. M. Lynch, J. L. Sessler, B. P. Hay, C.-H. Lee, *Angew. Chem.* **2008**, *120*, 5116 – 5120; *Angew. Chem. Int. Ed.* **2008**, *47*, 5038 – 5042; i) Z. R. Laughrey, T. G. Upton, B. C. Gibb, *Chem. Commun.* **2006**, 970 – 972.

[5] a) S. Lee, C.-H. Chen, A. H. Flood, *Nat. Chem.* **2013**, *5*, 704 – 710; b) Y. Li, A. Flood, *Angew. Chem.* **2008**, *120*, 2689 – 2692; *Angew. Chem. Int. Ed.* **2008**, *47*, 2649 – 2652; c) S. S. Zhu, H. Staats, K. Brandhorst, J. Grunenberg, F. Gruppi, E. Dalcanale, A. Lützen, K. Rissanen, C. A. Schalley, *Angew. Chem.* **2008**, *120*, 800 – 804; *Angew. Chem. Int. Ed.* **2008**, *47*, 788 – 792.

[6] G. Aullón, D. Bellamy, L. Brammer, E. A. Bruton, A. G. Orpen, *Chem. Commun.* **1998**, 653 – 654.

[7] F. Zordan, L. Brammer, P. Sherwood, *J. Am. Chem. Soc.* **2005**, *127*, 5979 – 5989.

[8] M. J. Mayoral, C. Rest, J. Schellheimer, V. Stepanenko, R. Albuquerque, G. Fernández, *J. Am. Chem. Soc.* **2013**, *135*, 2148 – 2151.

[9] OPEs are well-recognized to self-assemble in solution into various supramolecular structures. For recent examples, see: a) A. Gopal, M. Hifsudheen, S. Furumi, M. Takeuchi, A. Ajayaghosh, *Angew. Chem.* **2012**, *124*, 10657 – 10661; *Angew. Chem. Int. Ed.* **2012**, *51*, 10505 – 10509; b) A. Gopal, R. Varghese, A. Ajayaghosh, *Chem. Asian J.* **2012**, *7*, 2061 – 2067; c) F. García, L. Sánchez, *J. Am. Chem. Soc.* **2012**, *134*, 734 – 742; d) F. Wang, M. A. J. Gillissen, P. J. M. Stals, A. R. A. Palmans, E. W. Meijer, *Chem. Eur. J.* **2012**, *18*, 11761 – 11770; e) A. Florian, M. J. Mayoral, V. Stepanenko, G. Fernández, *Chem. Eur. J.* **2012**, *18*, 14957 – 14961; f) S. Mahesh, R. Thirumalai, S. Yagai, A. Kitamura, A. Ajayaghosh, *Chem. Commun.* **2009**, 5984 – 5986.

[10] For recent examples of amphiphilic Pt^{II} systems, see: a) L.-B. Xing, S. Yu, X.-J. Wang, G.-X. Wang, B. Chen, L.-P. Zhang, C.-H. Tung, L.-Z. Wu, *Chem. Commun.* **2012**, *48*, 10886 – 10888; b) J. Wang, Y. Chen, Y.-C. Law, M. Li, M.-X. Zhu, W. Lu, S. S.-Y. Chui, N. Zhu, C.-M. Che, *Chem. Asian J.* **2011**, *6*, 3011 – 3019; c) C. Po, A. Y.-Y. Tam, K. M.-C. Wong, V. W.-W. Yam, *J. Am. Chem. Soc.* **2011**, *133*, 12136 – 12143; d) W. Lu, Y. Chen, V. A. L. Roy, S. S.-Y. Chui, C.-M. Che, *Angew. Chem.* **2009**, *121*, 7757 – 7761; *Angew. Chem. Int. Ed.* **2009**, *48*, 7621 – 7625; e) V. W.-W. Yam, Y. Hu, K. H.-Y. Chan, C. Y.-S. Chung, *Chem. Commun.* **2009**, 6216 – 6218.

[11] Pt···Pt interactions are hindered if sterically bulky groups are attached to the Pt^{II} ion. For a recent example, see: X.-D. Xu, J. Zhang, L.-J. Chen, X.-L. Zhao, D.-X. Wang, H.-B. Yang, *Chem. Eur. J.* **2012**, *18*, 1659 – 1667.

[12] Sterically accessible Pt^{II} complexes self-assemble through metallophilic Pt···Pt interactions into supramolecular polymeric structures or gels. For recent Reviews, see: a) A. Y.-Y. Tam, V. W.-W. Yam, *Chem. Soc. Rev.* **2013**, *42*, 1540 – 1567; b) J. Zhang, C.-Y. Su, *Coord. Chem. Rev.* **2013**, *257*, 1373 – 1408; c) K. M.-C. Wong, V. W.-W. Yam, *Acc. Chem. Res.* **2011**, *44*, 424 – 434; d) M.-O. M. Piepenbrock, G. O. Lloyd, N. Clarke, J. W. Steed, *Chem. Rev.* **2010**, *110*, 1960 – 2004.

[13] The synthesis of ligand **1** is described in the Supporting Information.

[14] H.-J. Kim, T. Kim, M. Lee, *Acc. Chem. Res.* **2011**, *44*, 72 – 82.

[15] a) Z. Chen, A. Lohr, C. R. Saha-Möller, F. Würthner, *Chem. Soc. Rev.* **2009**, *38*, 564 – 584; b) T. F. A. De Greef, M. M. J. Smulders, M. Wolffs, A. P. H. J. Schenning, R. P. Sijbesma, E. W. Meijer, *Chem. Rev.* **2009**, *109*, 5687 – 5754; c) D. Zhao, J. S. Moore, *Org. Biomol. Chem.* **2003**, *1*, 3471 – 3491.

[16] When the ratio methanol/water is 60:40 or 50:50, the aggregate band at 372 nm does not fully transform into monomeric species upon heating, whereas at 80:20 only partial aggregation occurs (Figure S11).

[17] *Supramolecular Polymers*, 2nd ed. (Ed.: A. Ciferri), Taylor Francis, New York, **2005**.

[18] a) H. M. M. ten Eikelder, A. J. Markvoort, T. F. A. de Greef, P. A. J. Hilbers, *J. Phys. Chem. B* **2012**, *116*, 5291 – 5301; b) A. J. Markvoort, H. M. M. ten Eikelder, P. A. J. Hilbers, T. F. A. de Greef, E. W. Meijer, *Nat. Commun.* **2011**, *2*, 509 – 517.

[19] If a powder sample of **2** is directly dissolved in CD_3OD, initially a sharp ^1H NMR spectrum is observed. However, during the time required for ROESY studies (30–180 min) the solution becomes viscous because of the strong tendency of **2** to form gels and ultimately broad NMR signals are obtained (Figure S14a). To overcome this, **2** (18 mg) was dissolved in a minimum amount (0.05 mL) of CD_2Cl_2, followed by removal of the solvent until a dry film is formed and subsequent redissolution of the solid in 0.6 mL CD_3OD.

[20] O. V. Dolomanov, L. J. Bourhis, R. J. Gildea, J. A. K. Howard, H. Puschmann, *J. Appl. Crystallogr.* **2009**, *42*, 339 – 341.

[21] M. A. Spackman, D. Jayatilaka, *CrystEngComm* **2009**, *11*, 19 – 32.

[22] G. A. Jeffrey, *An introduction to hydrogen bonding*, 1st ed., OUP, Oxford, **1997**.

[23] Recently, related halogen-bonding interactions have been exploited for the construction of gels. See: L. Meazza, J. A. Foster, K. Fucke, P. Metrangolo, G. Resnati, J. W. Steed, *Nat. Chem.* **2013**, *5*, 42 – 47.

[24] G. R. Desiraju, *J. Am. Chem. Soc.* **2013**, *135*, 9952 – 9967.

